The impact of resin-coating on sub-critical crack extension in a porcelain laminate veneer material

Cao, Xu; Fleming, Garry J.p.; Addison, Owen

DOI:
10.1016/j.dental.2017.02.004

Document Version
Publisher's PDF, also known as Version of record

Citation for published version (Harvard):
Cao, X, Fleming, GJP & Addison, O 2017, 'The impact of resin-coating on sub-critical crack extension in a porcelain laminate veneer material', *Dental Materials*, vol. 33, no. 5, pp. 498-504. https://doi.org/10.1016/j.dental.2017.02.004

DENTAL MATERIALS 33 (2017) 498–504

Available online at www.sciencedirect.com

ScienceDirect

journal homepage: www.intl.elsevierhealth.com/journals/dema

The impact of resin-coating on sub-critical crack extension in a porcelain laminate veneer material

Xu Cao[a], *Garry J.P. Fleming*[b], *Owen Addison*[a,c,*]

[a] *Biomaterials Unit, University of Birmingham, School of Dentistry, 5 Mill Pool Way, Birmingham B5 7EG, UK*
[b] *Materials Science Unit, Dublin Dental University Hospital, Lincoln Place, Dublin 2, Ireland*
[c] *University of Alberta, School of Dentistry, Edmonton, AB, T6G 1C9, Canada*

ARTICLE INFO

Article history:
Received 21 September 2016
Received in revised form
14 February 2017
Accepted 16 February 2017

Keywords:
Veneer
Ceramic
Cement
Stress-corrosion
Strength

ABSTRACT

Objectives. Characterisation of the interaction between crack extension, crack stabilisation and stress/strain relaxation in the polymeric matrix, the interplay between stress corrosion cracking and the mechanical response of a resin-based luting adhesive within a surface defect population could extend PLV restoration longevity by optimising cementation protocols. The aim was to investigate the influence of stress corrosion cracking and the viscoelastic behaviour of a resin-based luting adhesive independently by controlling the environmental conditions operative during test specimen fabrication.

Methods. The effects of stress corrosion at ceramic crack tips and potential viscoelastic responses to loading of the resin-coated impregnating cracks were isolated. Resin-coated feldspathic ceramic test specimens were fabricated in ambient humidity or following moisture exclusion. Bi-axial flexure strengths of groups (n = 20) were determined at constant loading rates of 2.5, 10, 40, 160 or 640 N/min and data was compared with uncoated controls. Fractographic analyses were performed on all fractured test specimens.

Results. Resin-cement coating resulted in significant ceramic strengthening in all conditions tested ($p < 0.01$). A two-way ANOVA demonstrated that the exclusion of moisture during resin- coating significantly increased mean BFS ($p<0.01$) but post-hoc Tukey tests identified that moisture exclusion resulted in significant increases in BFS values only at intermediate loading rates with no significant differences observed at either the fastest or slowest loading rates (640 and 2.5 N/min, respectively).

Significance. Mechanical reinforcement of PLV materials by resin-cement systems is yet to be optimized. The viscoelastic behavior of the resin-cement itself can influence the magnitude of reinforcement observed and sub-critical crack growth.

1. Introduction

Porcelain Laminate Veneers (PLVs) are a minimally invasive treatment modality used routinely by dental practitioners to modify the esthetics of the anterior dentition [1]. The brittle nature of dental ceramics can result in the fracture of PLVs in service, despite often not being directly loaded through occlusal contact during function [2]. To address the mechanical deficiencies of PLV materials, efforts have been made using

* Corresponding author at: Biomaterials Unit, University of Birmingham, School of Dentistry, 5 Mill Pool Way, Birmingham B5 7EG, UK.
E-mail addresses: o.addison@bham.ac.uk, oaddison@ualberta.ca (O. Addison).
http://dx.doi.org/10.1016/j.dental.2017.02.004

in-vitro testing protocols to model the numerous variables that can influence PLV performance in-vivo [3–5]. Investigators have made comparisons with similar systems in the engineering literature where brittle coatings were intimately bonded to relatively compliant substrates namely, laminated glass and thermal barrier coatings [6–8]. To elucidate the key material, geometric, testing and environmental parameters that can determine the fracture pattern and associated strength values, investigators have predominantly employed methodological approaches which involve the indentation testing of ceramic materials bonded to an underlying substrate to form a bi-layered structure [6,9,10] or substrates that form multi-layered structures [10]. In indentation testing, the ceramic laminate or coating has been observed to fail due to Hertzian cone cracks propagating from the indentation contact zone (the surface in compression) or from the tensile extension of radial cracks originating at the opposite surface of the ceramic (the surface in tension) [6,11]. Radial crack extension is understood to be the dominant failure mechanism when the ceramic coating is thin and the supporting substrate is relatively compliant [6,10,11]. This failure mechanism has been demonstrated to predominate in the failure of PLVs in service [12,13].

Clinical survival data for PLV restorations identified that the highest fracture rate occur within the first year of service [14] which is often attributed to processing defects, errors in clinical decision making and/or technical execution. Despite the initial spike in early clinical failures, PLVs are routinely reported in the dental literature to have survival rates in excess of ten years [14,15]. Typically, PLVs are fabricated from amorphous glasses and glass-ceramics that are susceptible to stable crack growth, albeit over a considerable period of time, which can ultimately reduce the energetic requirement for catastrophic failure to occur [16,17]. In addition, PLVs are subject to forces of varying application rate, magnitude and frequency as part of normal masticatory function in-vivo. While the stable crack extension of defects in PLV materials is well understood, when ceramic materials are considered in isolation, it is essential to recognize that when employed clinically, the adhesive resin-based cement interacts directly with the ceramic surface defect population of the PLV restoration from which fracture originates [18]. The creation of tensile stress fields at the ceramic/resin-adhesive coating interface results in the extension of irregularities on the ceramic surface (defects, cracks or pores). This phenomenon is exacerbated in the presence of moisture by hydrolysis of the Si—O—Si bonds at the advancing crack tip, a process known as stress corrosion cracking or environmental assisted crack growth [19]. The polymeric matrix of the resin-based luting cement, which is chemically coupled to the ceramic surface by silane molecules and acts to stabilize against crack extension [20], is also simultaneously subjected to an equivalent applied tensile stress.

Polymeric materials are viscoelastic in nature, exhibiting a time-dependent plastic deformation such that during testing the mechanical properties of polymeric-based materials are sensitive to the rate of stress application [21]. The propensity for viscoelastic behavior in dental resin-based composite (RBC) materials is increased with reduced filler volume fraction and is therefore increased for flowable RBCs and resin-based luting adhesive systems compared with conventional dental RBC materials [21]. As a result, a balance between crack extension, crack stabilization and stress/strain relaxation in the polymeric matrix within the ceramic surface defect population must exist in response to the application of an applied load. Characterization of the interaction between crack extension, crack stabilization and stress/strain relaxation in the polymeric matrix, the interplay between stress corrosion cracking and the mechanical response of a resin-based luting adhesive within a surface defect population could extend PLV restoration longevity by optimizing cementation protocols. Therefore, the aim of the current study was to investigate the influence of stress corrosion cracking and the viscoelastic behavior of the resin-based luting adhesive by controlling the environmental conditions operative during test specimen fabrication. The strain-rate dependent behavior of both glassy ceramics and dental RBC materials have been previously characterized [17,22,23], thereby supporting the testing of an experimental hypothesis. The hypothesis tested was that in the absence of moisture, the strain-rate dependent behavior of a resin-based luting adhesive would dominate system strengthening.

2. Materials and methods

2.1. *Specimen manufacture*

To investigate the viscoelastic behavior of the resin-based luting adhesive, 50 resin-based adhesive (Rely-X Veneer Cement, shade A2, 3M ESPE, St. Paul MN, USA) bar-shaped specimens (25.0 ± 0.1 mm length, 2.0 ± 0.1 mm width, 2.0 ± 0.1 mm height) were fabricated by condensing the material into a Teflon mold. Following condensation of the adhesive, the mold was covered with an acetate strip, then a glass slide and finally a 1 kg weight were applied to ensure consistent specimen packing. The resin-based adhesive was light-irradiated with an overlapping irradiation protocol [24]. Firstly, the center of the specimen was irradiated through a 13 mm light curing unit (LCU) tip diameter, connected to an Optilux 501 (SDS Kerr, Danbury, CT, USA) LCU operating at an output intensity of 740 ± 38 mW/cm^2 for 20 s. The LCU tip diameter was moved such that the next irradiated area overlapped the previously exposed area by a quarter of the diameter of the exit window [24] and repeated until the entire specimen had been irradiated (three irradiations). To ensure consistency in the irradiation of the bar-shaped specimens the process was facilitated by pre-marking the acetate strip so that the LCU tip could be placed accurately. Following irradiation, the specimens were removed from the mold, checked for surface imperfections and any evidently defective specimens were replaced before light-irradiating the opposing surface using the overlapping protocol. All bar-shaped specimens were storage in a light excluding container for one week prior to flexural modulus determination.

A feldspathic dental ceramic (VITA VM7, Vita, Bad Säckingen, Germany) advocated for the manufacture of PLV restorations was used to produce 300 nominally identical disc-shaped specimens. A slurry mix consisting of 0.6 g of VITA VM7 base dentin powder (Lot 7433) and 0.22 mL of Vita Modelling Fluid (Lot 4209R) was manipulated and transferred to a Nylon ring mold (15.0 ± 0.1 mm diameter and 0.9 ± 0.1 mm

thickness), firmly secured to a base plate burnished with aluminum foil. A vibrating table (Croform Techniques Ltd, London, UK) was used to agitate the assembly for 90 s and excess liquid brought to the surface was repeatedly removed using absorbent tissues [25]. Following condensation, the surplus material was carefully removed from the overfilled mold with a razor blade prior to transferring the specimens to a flat silicon nitride sintering slab. The specimens were sintered according to the manufacturers' recommended firing cycle in a vacuum furnace (Vita Vacumat 40, Bad Säckingen, Germany), which involved preheating the samples to 500 °C (initial drying time) for 420 s before the temperature was increased at 55 °C/min to 910 °C under vacuum, held for 60 s and allowed to slow cool to room temperature.

The sintered disc-shaped specimens possessed both a 'glazed' surface formed by the condensation of the slurry onto the burnished aluminum and a 'fit' surface formed by the levelling of the alternate specimen surface with a razor blade. The 'fit' surfaces were hydrofluoric (HF) acid-etched for 90 s with 10% HF (Fisher Scientific UK Ltd, Loughborough, UK) and washed on five separate occasions (for 30 s intervals) in distilled water. After drying in an oil free air stream, the HF acid-etched surfaces were primed with 3-methacryloxypropyltrimethoxysilane (Rely-X Ceramic Primer, 3 M ESPE) and allowed to air dry (23 ± 1 °C and 50 ± 1% relative humidity) for 10 min. The 300 specimens were randomly assigned to 15 groups (n = 20). Groups A–E (n = 100 specimens) received no further surface treatment prior to bi-axial flexure strength (BFS) determination.

The remaining 200 specimens (Groups F–O) were transferred to a DAB 01S-P226 environmental chamber (Saffron Scientific Equipment Ltd., Knaresborough, UK). The 'fit' surfaces of the specimens from Groups F–J were resin-coated with Rely-X Veneer Cement under the ambient 'chair-side' environment (23 ± 1 °C and 50 ± 1% relative humidity). Using a calibrated dispenser, a consistent mass of the resin was applied to the center of the primed 'fit' surface of each disc-shaped specimen, covered with acetate and a glass slide and gently pressed manually until the resin spread to the disc periphery. The resin-coating was light-irradiated using the Optilux 501 LCU for 20 s at 740 ± 38 mWcm^{-2} with the 13 mm LCU tip diameter. The remaining specimens (Groups K–O) were resin-coated according to the protocol outlined for groups F–J specimens but with the environmental conditions adjusted to achieve an air moisture content of <1 ppm which was maintained by activation of the chamber's moisture depletion columns. The temperature and environmental gas composition during resin-coating were otherwise identical for all resin-coated specimens. Following resin-coating, the discs were stored for one week under ambient conditions (23 ± 1 °C and 50 ± 1% relative humidity) in a light excluding container prior to BFS testing and fractographic analyses.

2.2. Specimen testing

The three-point flexural moduli of the resin-based luting adhesive were calculated following seven day storage from the elastic segment of load-deflection plots generated by three-point flexure testing at constant loading rates of 2.5, 10, 40, 160 or 640 N/min (n = 10 per loading rate). The flexural moduli (E_2) were calculated in accordance with ISO 4049 [26] where

$$E_B = \frac{PL^3}{4bd^3D} \tag{1.1}$$

and P was the load at failure, L the support span (20 mm), b the specimen width, d the specimen thickness and D the deflection.

The BFS of the disc-shaped specimens was determined in a ball-on-ring configuration by placing the specimens on a 10 mm diameter stainless steel support-ring with the upper 'glazed' surfaces centrally loaded with a 4 mm diameter stainless steel spherical ball indenter. Disc-shaped specimens were tested at 2.5 N/min (Groups A, F and K), 10 N/min (Groups B, G and L), 40 N/min (Groups C, H and M), 160 N/min (Groups D, I and N) and 640 N/min (Groups E, J and O). Multi-layered bi-axial solutions were employed to calculate the BFS value at the locus of failure, namely the 'fit' surface of the ceramic specimens [27]. The neutral axis of bending (t_n) was calculated (Eq. (1.2)) as a function of the thicknesses of the ceramic (t_1) and the resin-coating (t_2). The elastic modulus of the feldspathic dental ceramic (E_1) was 68 GPa [26] and the elastic modulus of the resin-based luting adhesive (E_2) was experimentally determined for each loading rate (Eq. (1.1) as described earlier). ν_1 and ν_2 were the Poisson's ratios of the ceramic (0.25 [28]) and resin (0.27 [29]), respectively.

$$t_n = \frac{E_1^*(t_1)^2 - E_2^*(t_2)^2}{2(E_1^*t_1 + E_2^*t_2)} \tag{1.2}$$

and

$$E^* = \frac{E}{1-\nu^2} \tag{1.3}$$

The BFS values were calculated at the center of the disc-shaped specimens at axial positions throughout the specimen thickness (z), where the bonded interface was located at z = 0, the ceramic surface at z = t_1 and the resin surface at z = $-t_2$, for ($0 \le z \le t_1$),

$$\sigma = \frac{-3P(1+\nu)(z-t_n)}{2\pi(t_1+t_2)^3}\left[1+2\ln\left(\frac{a}{b}\right)+\frac{1-\nu}{1+\nu}\left(1-\frac{b^2}{2a^2}\right)\frac{a^2}{R^2}\right]\left[\frac{E_1^*\left(E_1^*t_1+E2^*t_2\right)(t_1+t_2)^3}{\left(E_1^*t_1^2\right)^2+\left(E_2^*t_2^2\right)^2+2E_1^*E_2^*t_1t_2\left(2t_1^2+2t_2^2+3t_1t_2\right)}\right] \tag{1.4}$$

and for ($-t_2 \le z \le 0$),

$$\sigma = \frac{-3P(1+\nu)(z-t_n)}{2\pi(t_1+t_2)^3}\left[1+2\ln\left(\frac{a}{b}\right)+\frac{1-\nu}{1+\nu}\left(1-\frac{b^2}{2a^2}\right)\frac{a^2}{R^2}\right]\left[\frac{E_2^*\left(E_1^*t_1+E_2^*t_2\right)(t_1+t_2)^3}{\left(E_1^*t_1^2\right)^2+\left(E_2^*t_2^2\right)^2+2E_1^*E_2^*t_1t_2\left(2t_1^2+2t_2^2+3t_1t_2\right)}\right] \tag{1.5}$$

where,

$$\nu = \frac{(\nu_1 t_1 + \nu_2 t_2)}{t_1 + t_2} \quad (1.6)$$

P was the load at fracture, a, b and R were the radii of the knife-edge support, loaded region and specimen, respectively. For the uncoated specimens (when $t_2 = 0$) the expression resolves to a monolayer solution for BFS of disc-shaped specimens bending in a ball-on-ring configuration [30].

2.3. Statistical analyses

Initially, a two-way analysis of variance (ANOVA) was employed to identify differences in the mean BFS values of the uncoated specimens and specimens resin-coated under ambient conditions ($\alpha = 0.05$: factors = resin-coating at two levels; loading rate at five levels). Subsequently, a further two-way ANOVA and post-hoc Tukey tests were used to identify differences in the mean BFS values of specimens' resin-coated in ambient or moisture depleted environments ($\alpha = 0.05$: factors = environmental condition at two levels; loading rate at five levels). The relationship between BFS and loading rate and flexural modulus and loading rate were explored using regression analyses.

2.4. Fractographic analyses

All fracture fragments from the 300 specimens tested under the BFS protocols were imaged in a scanning electron microscope (SEM; EVO, Carl Zeiss, Germany) in backscattered electron imaging mode under low vacuum at 20 kV to identify both the fracture origins and the pattern of failure in accordance with standard fractographic principles.

3. Results

The mean flexural moduli and associated standard deviations of the Rely-X Veneer bar-shaped specimens were 6.87 (0.38), 7.00 (0.58), 7.52 (0.58), 7.88 (0.67) and 7.95 (0.64) GPa at loading rates of 2.5, 10, 40, 160 or 640 N/min, respectively (Fig. 1a). The mean elastic modulus at each stress rate were used as the definite value of E_2 in Eqs. (1.2)–(1.5) to calculate the BFS values of the resin-coated disc-shaped test specimens.

The two-way ANOVA confirmed significant strengthening due to resin-coating of the ceramic substrate ($p < 0.01$). The loading rate applied during testing also significantly impacted on the mean BFS values with an increase in mean BFS values observed with increasing loading rate ($p < 0.01$), but the effect was not influenced by the presence or absence of the resin-coating ($p = 0.49$). A further two-way ANOVA identified that the exclusion of moisture during resin-coating significantly increased the mean BFS values ($p < 0.01$), however, there was no significant interaction between loading rate and the environmental processing conditions on the mean BFS ($p = 0.57$). Post-hoc Tukey tests identified that at the fastest loading rate (640 N/min) no significant difference was observed in the mean BFS values of specimen's resin-coated in an ambient or moisture depleted environment (Fig. 1b). Additionally, at the slowest loading rate (2.5 N/min), minimal differences in the mean BFS values of specimen's resin-coated in an ambient or moisture depleted environment were observed (Fig. 1b).

Scanning electron microscopy identified that failure in all resin-coated BFS specimens originated at the 'fit' surface of the ceramic under maximum tensile stress fields during BFS testing (Fig. 2). The presence of porosity within the resin-coating and the size of the ceramic surface defects strongly correlated with the magnitude of resin-strengthening observed irrespective of the loading and resin-coating conditions (Fig. 2a–c). Specimens which exhibited no apparent porosity in the vicinity of the fracture origin produced the highest BFS values (Fig. 2a) and specimens associated with resin-coating porosity near a large ceramic surface defect or imperfection recorded the lowest BFS values (Fig. 2c). Interestingly, for a number of specimens tested at 0.25 N/min, clear surface damage originating from the ball-indentor loading site were observed and the pattern was macroscopically consistent with a Hertzian cone fracture (Fig. 3a). However, further fractographic analyses identified that the phenomenon was a secondary event subsequent to tensile failure, confirmed as the Hertzian cone cracks transect the wake hackles from a preceding radial fracture event (Fig. 3b).

4. Discussion

The relationship between the loading rate (proxy for stressing rate) and the mean BFS values for the uncoated ceramic appeared close to log-linear, with the mean BFS value increasing with increasing loading rate, a phenomenon ascribed to the reduction in time available for stress corrosion cracking prior to catastrophic failure [19,31]. In agreement with previously reported data [32], resin-coating significantly increased the mean BFS of the PLV ceramic at all stressing-rates investigated. It is noted that in the clinical situation, irrespective of the cementation conditions, resin-based cements will transport water to the ceramic surface so that crack tip hydrolysis will be inevitable. In the current study, the effect of water sorption into the resin-cement was excluded as factor, as its influence on the elastic and viscoelastic responses of the cement itself, would have masked subtle modifications to stress-corrosion behavior [22]. The log-linear relationship between increasing stressing-rate and mean BFS value was largely maintained ($BFS_{coated} = 4.99\ln(rate) + 106$ and $BFS_{uncoated} = 4.41\ln(rate) + 67$) following resin-based luting adhesive application, when resin-coating was performed in ambient humidity conditions. The finding implied that stress corrosion cracking (crack tip hydrolysis) conditions were maintained at the ceramic surface irrespective of the presence of the resin-based luting adhesive coating, which supports accepting the experimental hypothesis. It is clear, however, that the proportional mean BFS increase conferred by resin-coating was largely independent of the stressing-rate during testing. These observations led to the rejection of the previously reported theory [33] that the observed reinforcement conferred to dental ceramics by adhesive cementation (resin-coating) was a result of moisture exclusion at the crack tip of critical surface defects [33]. Indeed, even when moisture depletion to an air moisture content of <1 ppm was achieved, the additional mean BFS increase was minor and resulted

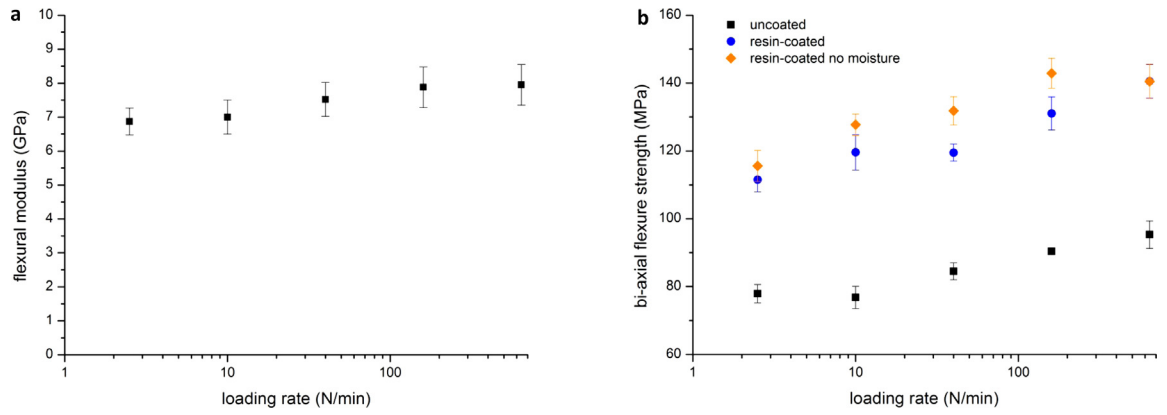

Fig. 1 – (a) Plot of loading rate (log scale, N/min) against mean flexural modulus (GPa) derived from the three-point flexure testing of Rely-X Veneer bar-shaped specimens loaded at 2.5, 10, 40, 160 and 640 N/min. (b) Plot of loading rate (log scale, N/min) against mean BFS value when tested at loading rates of 2.5, 10, 40, 160 and 640 N/min, for uncoated ceramic specimens and resin-coated specimens without and with moisture exclusion during specimen manufacture. (Error bars reflect ±1 standard deviation.)

in only a small modification to the pattern of the BFS data which may be attributed to the behavior of the polymer itself [21,22]. The testing conditions employed provide insight into stress-corrosion under fixed stressing-rate conditions. in-vivo exposure of PLVs to cyclic loading can modify the influence of water at surface defects further introducing the potential for hydraulic effects [6].

The analytical solutions used [27], confirmed the stress maxima in the resin-based luting adhesive coating remained well under the elastic limit of the luting adhesive, such that failure could not have arisen from within the resin-layer and this was further confirmed fractographically. It has been established in the literature that the flexural modulus of RBC materials decreases with stressing rate (and vice versa) which indicates that stress relaxation mechanisms are operative during mechanical loading [22]. Additionally, the application of sustained loading has previously been highlighted to lead to internal flow and/or chain segment relaxation within the polymeric network [21,22]. In the current study, the mean flexural modulus of the resin-based luting adhesive increased with increasing stressing rate (from 2.5 to 160 N/min) followed by the appearance of a plateau region between 160 and 640 N/min which again was in agreement with the dental literature [22]. However, it should be noted that at the individual ceramic defect level, constraint of the polymer within individual cracks leads to an increase in the effective stiffness of the polymeric material [29,34,35] and the sensitivity to stressing-rate under these condition could not be directly assessed. Unsurprisingly at high stressing rates (160 and 640 N/min), where there was little available time for stress corrosion cracking (crack tip hydrolysis) to occur, environmental moisture conditions had no impact on the BFS data. At low stressing rates where time was available for stress corrosion cracking to occur, no significant additional resin-coating strengthening was observed. This finding indicated the strengthening mechanism by which the resin-based luting adhesive coating conferred reinforcement must also have been decaying under these specific conditions. Stress relaxation in the polymer will occur and

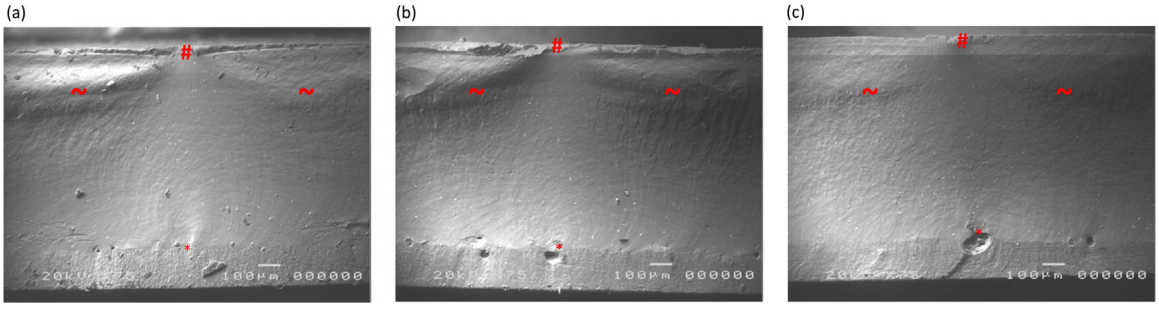

Fig. 2 – Scanning electron micrographs of representative fracture fragments derived from BFS testing. The load indentation site is demonstrated as (#), a typical compression curl is seen subsurface close to the loaded surface (~) and the fracture origin (*) lies at the contralateral lower surface either directly or slightly radially positioned relative to the loading axis. (a) exhibits an intimate interface between the resin-based luting adhesive and the ceramic surface with no obvious porosity evident and recorded a BFS value of 168 MPa (high); (b) exhibits porosity within the resin-based luting adhesive, close to the fracture origin, but not intimately connected to the ceramic surface and recorded a BFS value close to the mean BFS value (144 MPa); and (c) exhibited large porosity at the resin-based luting adhesive interface with the presence of a large pre-existing defect within the ceramic surface and recorded a BFS value of 92 MPa (low).

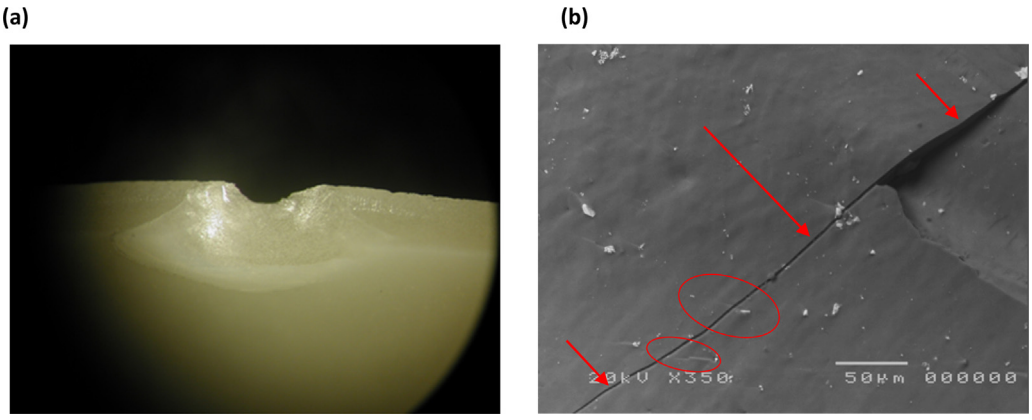

Fig. 3 – (a) Optical image of a specimen fracture fragment and (b) scanning electron micrograph of the fracture surface of a representative resin-coated ceramic specimen tested under BFS loading conditions at 2.5 N/min. For this testing regimen only a number of specimens exhibited material loss from the upper loaded surface during the fracture event consistent with Hertzian dominated fracture originating at the loading zone. Fractographic analysis showed that Hertzian fracture was secondary to initial radial fracture and that the fracture origin remained at the opposing ceramic resin-coated ceramic interface. The scanning electron micrograph demonstrates the fracture face showing the Hertzian crack (indicated by arrows) bisecting pre-formed wake Hackles formed in the initial radial fracture event.

when combined with any loss of adhesion between the resin-based luting adhesive coating and the ceramic surface would account for the observations. Importantly and irrespective of the stressing-rate, within the samples groups investigated, specimens that yielded low BFS values were associated with porosity at the resin-based luting adhesive coating/ceramic interface (Fig. 2c) which cause subtle changes in the distribution of the BFS data (Fig. 1b). It is evident that under the loading conditions (proxy for stressing rate), the strength limiting defect of the system is a function of the statistical likelihood of encountering a loss of reinforcement across the defect integral rather than the application of the Griffith criterion [36] in isolation.

5. Conclusion

The significance of the current findings is that mechanical reinforcement of PLV materials by resin-based adhesive luting systems are not optimized. When PLVs are employed clinically, stress corrosion cracking (crack tip hydrolysis) appears to be inevitable as a result of water sorption by the resin, notwithstanding the presence of moisture at the crack tips of ceramic surface defects. However, resin-based adhesive luting systems which exhibit reduced viscoelasticity and increased flexural moduli should be explored in combination with improvements in the predictability of wetting of the ceramic surface by resin-based adhesive luting systems, to prevent the entrapment and subsequent inclusion of strength limiting porosities.

Acknowledgement

This work was supported by the Engineering and Physical Sciences Research Council, UK. Grant code: EP/H028617/1.

REFERENCES

[1] Faunce FR, Myers DR. Tooth restoration with porcelain laminate veneers. J Tex Dent Assoc 1977;53:30–2.
[2] Beier US, Kapferer I, Burtscher D, Dumfahrt H. Clinical performance of porcelain laminate veneers for up to 20 years. Int J Prosthodont 2012;25:79–85.
[3] Fleming GJP, Hooi PA, Addison O. The influence of resin flexural modulus on the magnitude of ceramic strengthening. Dent Mater 2012;28:769–76.
[4] Lin TM, Liu PR, Ramp LC, Essig ME, Givan DA, Pan YH. Fracture resistance and marginal discrepancy of porcelain laminate veneers influenced by preparation design and restorative material in vitro. J Dent 2012;40:202–9.
[5] Stappert CF, Ozden U, Gerds T, Strub JR. Longevity and failure load of ceramic veneers with different preparation designs after exposure to masticatory simulation. J Prosthet Dent 2005;94:132–9.
[6] Chai H. Crack propagation in glass coatings under expanding spherical contact. J Mech Phys Solids 2006;54:447–66.
[7] Chai H, Lawn BR. Failure of brittle layers on polymeric substrates from Vickers indentation. Scr Mater 2006;55:335–8.
[8] Chai H, Lawn BR, Wuttiphan S. Fracture modes in brittle coatings with large interlayer modulus mismatch. J Mater Res 1999;14:3805–17.
[9] Kim HW, Deng Y, Miranda P, Pajares A, Kim DK, Kim HE, et al. Effect of flaw state on the strength of brittle coatings on soft substrates. J Am Ceram Soc 2001;84:2377–84.
[10] Lawn BR, Bhowmick S, Bush MB, Qasim T, Rekow ED, Zhang Y. Failure modes in ceramic-based layer structures: a basis for materials design of dental crowns. J Am Ceram Soc 2007;90:1671–83.
[11] Wang Y, Darvell BW. Failure mode of dental restorative materials under Hertzian indentation. Dent Mater 2007;23:1236–44.
[12] Karlsson S, Landahl I, Stegersjö G, Milleding P. A clinical evaluation of ceramic laminate veneers. Int J Prosthodont 1992;5:447–51.

[13] Dumfahrt H, Schäffer H. Porcelain laminate veneers. A retrospective evaluation after 1 to 10 years of service: part II-clinical results. Int J Prosthodont 2000;13:9–18.
[14] Burke FJT, Lucarotti PS. Ten-year outcome of porcelain laminate veneers placed within the general dental services in England and Wales. J Dent 2009;37:31–8.
[15] Layton DM, Clarke M, Walton TR. A systematic review and meta-analysis of the survival of feldspathic porcelain veneers over 5 and 10 years. Int J Prosthodont 2012;25:590–603.
[16] Joshi GV, Duan Y, Della Bona A, Hill TJ, St John K, Griggs JA. Contributions of stress corrosion and cyclic fatigue to subcritical crack growth in a dental glass-ceramic. Dent Mater 2014;30:884–90.
[17] Gonzaga CC, Cesar PF, Miranda Jr WG, Yoshimura HN. Slow crack growth and reliability of dental ceramics. Dent Mater 2011;27:394–406.
[18] Addison O, Marquis PM, Fleming GJP. Adhesive luting of all-ceramic restorations—the impact of cementation variables and short-term water storage on the strength of a feldspathic dental ceramic. J Adhes Dent 2008;10:285–93.
[19] Wiederhorn SM, Bolz LH. Stress corrosion and static fatigue of glass. J Am Ceram Soc 1970;53:543–8.
[20] Addison O, Marquis PM, Fleming GJP. Quantifying the strength of a resin-coated dental ceramic. J Dent Res 2008;87:542–7.
[21] Baroudi K, Silikas N, Watts DC. Time-dependent visco-elastic creep and recovery of flowable composites. Eur J Oral Sci 2007;115:517–21.
[22] Musanje L, Darvell BW. Effects of strain rate and temperature on the mechanical properties of resin composites. Dent Mater 2004;20:750–65.
[23] Gonzaga CC, Cesar PF, Miranda Jr WG, Yoshimura HN. Determination of the slow crack growth susceptibility coefficient of dental ceramics using different methods. J Biomed Mater Res B: Appl Biomater 2011;99: 247–57.
[24] Bhamra GS, Fleming GJP. Effects of halogen light irradiation variables (tip diameter, irradiance, irradiation protocol) on flexural strength properties of resin-based composites. J Dent 2008;36:643–50.
[25] Fleming GJP, Shaini FJ, Marquis PM. An assessment of the influence of mixing induced variability on the bi-axial flexure strength of dentine porcelain discs and the implications for laboratory testing of porcelain specimens. Dent Mater 2000;16:114–9.
[26] ISO 4049. (E) Dentistry, polymer based filling restorative and luting materials. International Organisation for Standardisation; 2000.
[27] Hsueh CH, Lance MJ, Ferber MK. Stress distributions in thin bilayer discs subjected to ball-on-ring tests. J Am Ceram Soc 2005;88:1687–90.
[28] Zeng K, Odén A, Rowcliffe D. Evaluation of mechanical properties of dental ceramic core materials in combination with porcelains. Int J Prosthodont 1988;11:183–9.
[29] De Jager N, Pallav P, Feilzer AJ. The apparent increase of the Young's modulus in thin cement layers. Dent Mater 2004;20:457–62.
[30] Shetty DK, Rosenfield AR, McGuire P, Duckworth WH. Biaxial flexure test for ceramics. Ceram Bull 1980;59:1193–7.
[31] Glathart JL, Preston FW. The fatigue modulus of glass. J Appl Phys 1946;17:189–95.
[32] Hooi P, Addison O, Fleming GJP. Testing rate and cementation seating load effects on resin-strengthening of a dental porcelain analogue. J Dent 2013;41:514–20.
[33] Nathanson D. Principles of porcelain use as an inlay/onlay material. In: Garber DA, Goldstein RE, editors. Porcelain and composite inlays and onlays: esthetic posterior restorations. Chicago: Quintessence; 1993. p. 23–32.
[34] Addison O, Marquis PM, Fleming GJP. Resin elasticity and the strengthening of all-ceramic restorations. J Dent Res 2007;86:519–23.
[35] Wang FH, Hand RJ, Ellis B, Seddon AB. Glass strengthening using epoxy coatings. Phys Chem Glasses 1995;36:201–5.
[36] Griffith AA. The phenomena of rupture and flow in solids. Philos Trans R Soc A 1921;221:163–98.